

Properties of Recycled Fuels; Density Functional Theory Study

B. Szpunar¹, J.A. Szpunar²

¹Department of Physics and Engineering Physics
University of Saskatchewan, Saskatoon, Canada
B.Szpunar@usask.ca

²Department of Mechanical Engineering
University of Saskatchewan, Saskatoon, Canada

Abstract

The application of *Density Functional Theory (DFT)* approximation to assess the mechanical and structural properties of recycled urania and thoria fuel is presented. The calculated values of the lattice constant and mechanical moduli of ThO₂ and UO₂ are in good agreement with the experimental data. The calculations are further extended to study lattice constants of Pu-U oxides for which we do not have currently experimental data. The presented elastic moduli of ThO₂, UO₂ and Pu-U oxides are compared. The relative changes of the lattice constant of thoria and urania, calculated by first principles molecular dynamics as a function of temperature, agree with experiment.

1. Introduction

At the time of increasing cost of traditional urania fuel, it is more economically justified to look at the alternative fuels like thoria [1] or recycled fuel, mixed oxides, that contains Pu [2]. It is also of interest to reduce nuclear waste and burn Pu. The spent fuel of light water reactors (LWR) contains about 0.9 wt% U-235 and 0.6% fissile plutonium, which exceed the fissile content (0.7% U-235) of natural uranium. Therefore, such fuel can be used in CANDU reactors and this technology was developed very early [3]. The recycled fuel from LWR is called DUPIC, because it does not require any enrichment. The oxidation and reduction cycle (OREOX) was used to break fuel sheath due to increasing stress caused by the expansion of oxidized fuel (U₃O₈) [3]. This process is also used to produce the powdered uranium oxide for fuel pellet production. After final reconditioning, the reprocessed fuel can be sintered as described in reference [3].

The following paper discusses the application of *Density Functional Theory (DFT)* to assess the mechanical and structural properties of recycled urania and thoria fuel. Detailed calculation of the crystallographic lattice structure and mechanical properties of new fuel materials complement experimental measurements, and they also enhance our understanding of the structural properties of the fuels used in nuclear reactors.

The CASTEP *first-principles* quantum mechanical program, employing density functional theory [4], is commonly used to study the structure and properties of materials. The CASTEP code uses pseudopotentials and it has been already demonstrated [5] that plane wave ultrasoft

pseudopotentials predict structural properties of various compounds, containing lanthanides and actinides, in agreement with experiments.

Using the total energy minimization method [4], the equilibrium lattice constants, and the positions of atoms in pure, doped urania and thoria can be calculated. The current calculations were performed for idealized structures with small unit cells. Such small unit cells are convenient to use in the *first-principles* methods simulations, since the demand on computational resources is reduced.

The structural optimization according to the Broyden–Fletcher–Goldfarb–Shanno (BFGS) of the total energy minimization is used [4]. This minimization is performed using iterative methods, when forces and stresses are minimized (almost vanish), within the limit of the total energy pseudopotentials method and the equilibrium lattice constants and the positions of atoms of stoichiometric thoria and urania are calculated. The calculated values of the lattice constant of ThO₂ and UO₂ agree with the experimental data. Then the CASTEP *first-principles* calculations were used to study lattice constants of Pu-U oxides for which experimental values are not available in the literature. The elastic constants calculations are presented for single crystals of ThO₂, UO₂ and Pu-U oxides. The experimental values of elastic moduli pertain to a grain aggregate where grains have randomly orientated crystallographic directions and this assumption applies to calculation of bulk (B), shear (G) and Young moduli.

2. Structure of U-Th-Pu oxides

The CASTEP *first-principles* calculations of lattice constants for various uranium oxides and gadolinium compounds were presented in the reference [6]. In the previous calculations for various actinide oxides [5, 6] the electronic exchange-correlation potential was approximated within the Generalized Gradient Approximation (GGA) framework [7, 8]. The GGA calculations predict that UO₂ is metallic because ⁵f band of uranium does not split. It is found that the band splitting occurs when the Hubbard U correction is included for ⁵f electrons of uranium (implemented as in Ref. [9]) and the calculated band gap is linearly dependent on the value of U. Local density approximation (LDA) is used here since we confirm that the GGA overestimate bond lengths [10] and therefore predicts too small elastic moduli [11,12].

The structure of urania, thoria and Pu doped urania are shown in Figure 1.



Figure 1 Lattice structure of pure urania and thoria (a) and mixed fuel (b) with Plutonium (25% atomic substitution of U). Uranium, thorium, plutonium and oxygen atoms are marked as spheres, with the radius ranging from the largest for U and Th atoms to the smallest for O atoms.

Table 1 presents a comparison of our previous calculations [6] of lattice constant (GGA used) of urania with the calculations [12,13] where LDA [14] is used and the new calculation within LDA + U [9] approximation. The LDA calculations were performed for U-Th-Pu oxides.

Table 1
 Lattice constants, spins, electronic charges (on oxygen atoms) and energies (per non-oxygen atom) calculated using CASTEP [4].

Compound	Structure	Energy per non-O atom [eV]	Method	Spin (U/Th)	Spin (Pu)	Lattice constants (a) [nm]	Charge (O) [electron]
UO ₂	Fm $\bar{3}m$	-30.71	GGA	1.18		0.545	-0.65
UO ₂	Fm $\bar{3}m$	-30.71	LDA	1.15		0.533	-0.60
ThO ₂	Fm $\bar{3}m$	-31.73	LDA	0.00		0.553	-0.69
ThO ₂	Fm $\bar{3}m$	-29.33	GGA	0.00		0.558	-0.73
UO ₂ LDA+U	Fm $\bar{3}m$	-31.30	LDA + U (U = 2 eV)	1.07		0.543	-0.67
UO ₂ LDA+U	Fm $\bar{3}m$	-30.51	LDA + U (U = 3.5 eV)	1.07		0.548	-0.67
PuU ₃ O ₈	Pm $\bar{3}m$	-33.13	LDA	1.04	2.56	0.533	-0.58

The experimentally measured lattice constant of pure urania at 399K is 0.54582 nm [15]. Before comparing this experimental value with the calculated value at 0 K, the experimental value should be reduced by about 0.002 nm to compensate for thermal expansions.. U value equal to 2 eV for ⁵f electrons of uranium, leads to the lattice constant value (0.543 nm) that is in a very good agreement with the reduced value at 0 K. Presented in Table 1, lattice constants for pure urania calculated using LDA and LDA + U (3.5 eV) also agree well with the experimental measurements and the calculated previously value, 0.5458 nm [5], using GGA. While GGA and LDA + U (with commonly used higher U values to fit band gap; e.g. 3.5 eV for which a = 0.5458 nm) calculations predict slightly larger lattice constant, the value predicted by LDA is underestimated. The experimental value of the lattice constant of ThO₂ (0.55997 nm) [15] is slightly underestimated in the presented LDA (at 0 K) calculations (0.553 nm), while larger value (Table 1) obtained using GGA (0.558 nm) agrees very well with the experiment.

The magnetic properties of uranium oxides were discussed in details in Reference [6]. The presented calculations (Table 1), using Mulliken analysis, show that the calculated spin value of uranium is slightly lower when LDA is used. The charge transfer to oxygen, which is shown in the last column of Table 1, is only slightly lower when LDA is used and it is even less affected by Pu substitution.

In Figure 2 the band structure of ThO₂ (LDA) and UO₂ (LDA + U (2 eV)) are shown with the indicated band gaps (along the presented path in k space): 4.817 eV and 2.228 eV, respectively. These band gaps are slightly larger than calculated band gaps for all used k points: 4.511 eV (4.615 eV for GGA calculations) and 2.014 eV, respectively. The band gap of urania for LDA + U (3.5 eV) implementation agrees very well with the experiment (2.1 eV [17]). However, the U value (3.5 eV) that reproduces the optical band gap of urania, overestimates the lattice constant (see Table 1).

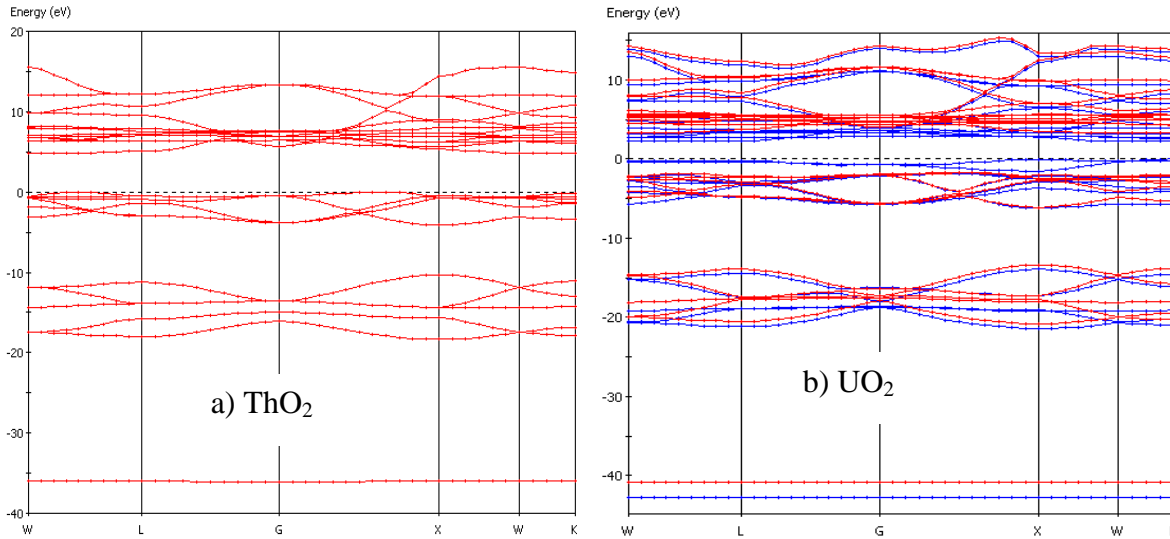


Figure 2 The band structure of thorium (a) and pure uranium (b) calculated using LDA and LDA + U (3.5 eV) respectively. The blue lines indicate band structure of electrons that have spins along the direction of majority spin.

3. Elastic properties of U-Th-Pu oxides

The experimental values of elastic moduli pertain to a grain aggregate (where grains have randomly orientated crystallographic directions) rather than to a single crystal. A completely random orientation of the grains is assumed in the computation. The formulas of Reuss [18] (R) and Voigt [19] (V) are employed in these computations of elastic moduli. These formulas provide the lower upper-bound and the higher lower-bound values for the polycrystalline aggregate. The final values of moduli are calculated as an average over R and V moduli and the details on this calculation can be found in [13]. Since in the Reference [5] only the elastic constants were presented, the derived moduli B, G and Y presented in Table 2, are calculated using Voigt approach only (c_{ij} are elastic constants):

$$B_V = (A + 2B)/3, G_V = (A - B + 3C)/5, Y_V = 9B_V G_V / (3B_V + G_V) \quad (1)$$

where:

$$\begin{aligned} 3A &= c_{11} + c_{22} + c_{33} \\ 3B &= c_{23} + c_{31} + c_{12} \\ 3C &= c_{44} + c_{55} + c_{66} \end{aligned} \quad (2)$$

In the present work we performed calculations of the elastic constants for U-Th-Pu oxides using the most recent version of CASTEP (5.5). The calculations for new LDA + U functional are also shown for UO₂ in Table 2.

As it can be seen in Table 2a, the calculations that use the LDA or the LDA + U approximations agree better with the measured [20] elastic moduli of UO₂ than when GGA/PBE [5] is implemented. The bulk moduli for LDA + U approximation were calculated using p-V cubic relation (illustrated in Figure 3) and as shown in Table 2a the values (214 GPa and 216 GPa for the Hubbard U values equal to 2 and 3.5 eV, respectively) agree very well with the experimental value (208.9 GPa [17]).

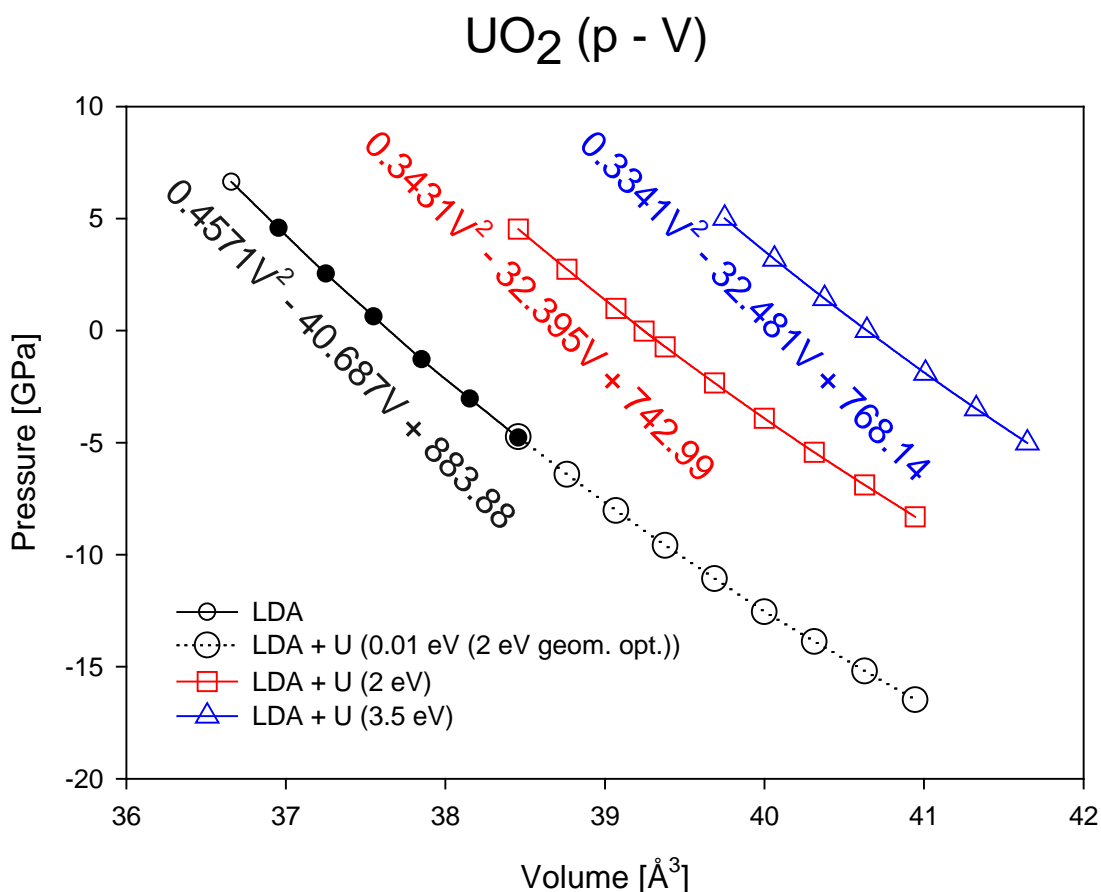


Figure 3 The p – V cubic relation, derived from CASTEP calculations within LDA + U scheme, as a function of U.

The Hubbard U term mainly shifts energy curves, therefore the stress strain gradients for the elastic moduli for U equal 2 eV (shown in Table 2a in column 5) were calculated using LDA+U geometries, but with Hubbard term omitted, as it creates too big noise in statistical fitting [21]. Alternatively to eliminate the effect of observed noise (as shown by square symbols in Fig. 4 for 0.009 strain), in stress strain curves for U equal to 3.5 eV, larger strains (maximum strain 0.09) than used in LDA calculations (maximum strain 0.003) were applied as illustrated in Figures 4 a,b.

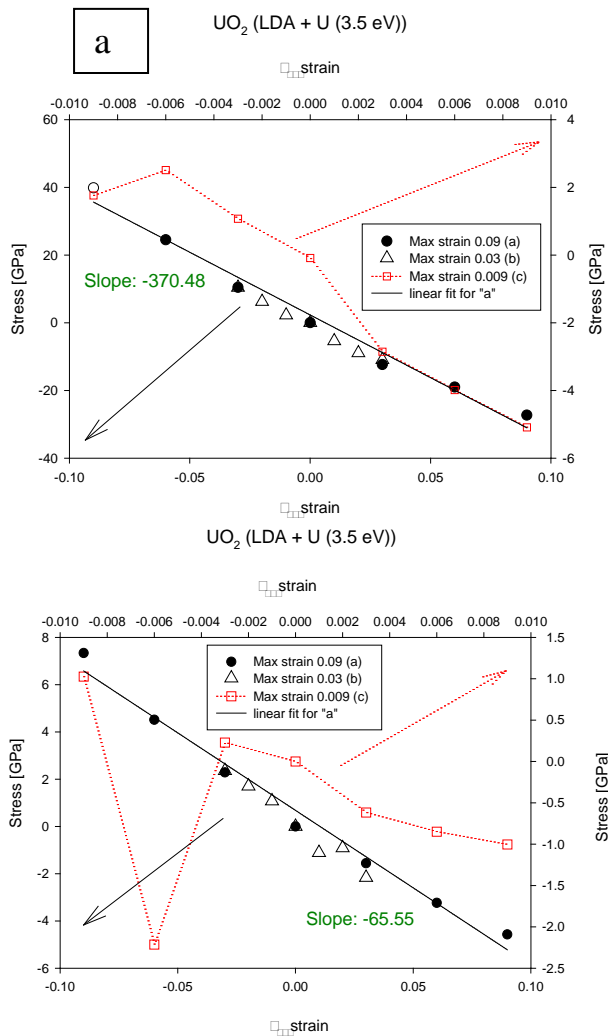


Figure 4 The stress-strain relation derived from CASTEP (LDA + U (3.5 eV)) calculations for (a) ϵ_{11} and (b) ϵ_{44} strains, respectively. The arrows points to the axes relevant to the plot since the additional (top and right axes) are added for 0.009 strain.

The shown in Table 2a results (6th column) were consistent with the repeated calculations for three times lower strain (0.03) and the calculated elastic moduli (c_{11} and c_{44}) from the second derivative of energy (7th column in Table 2 a). In Figure 5 the calculated energy (per UO_2) is

shown as a function of ϵ_{11} strain (coinciding with the [100] Hubbard U quantization axis). In this case the perfect ($R^2 = 1$) parabolic fit was found, although the pressure values were not reliable. In Table 2a (last column) c_{11} constant was derived from Eq. 1 and c_{44} elastic constant (used share: perpendicular to the Hubbard U quantization axis) was calculated from the fitted parabolic relation (energy versus strain) as described above. However when we applied respective strains to obtain shear constant $((c_{11} - c_{12})/2)$ the big noise in both the energy and pressure was observed. The inclusion of a Hubbard U correction to 5f electrons of uranium changes urania from a metal to an insulator and, therefore, has a dramatic effect on the localisation of the electron spin and charge density on uranium. The shown in Fig. 4 of Ref. [21] associated peaks lead to the observed noise in the pressure and energy for some deformations.

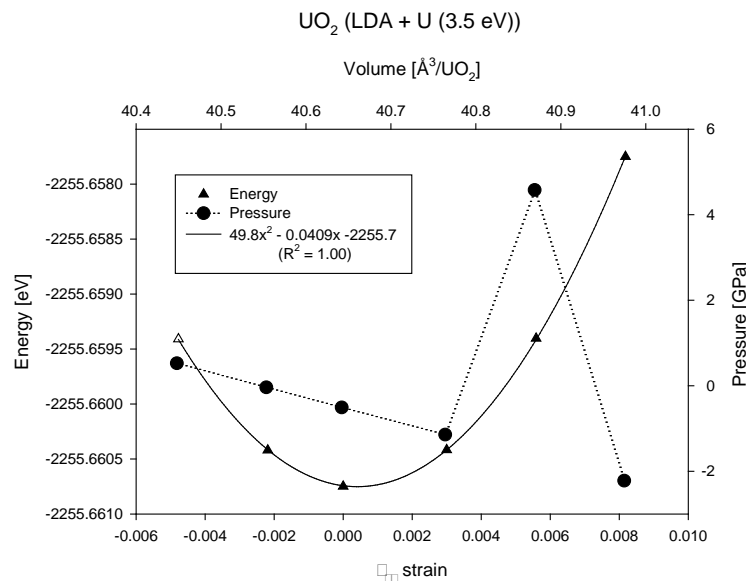


Figure 5 Energy- ϵ_{11} strain relation derived from CASTEP (LDA + U (3.5 eV)) calculations. The arrows points to the axes relevant to the plot since the additional top and right axis are added for pressure strain relation.

Table 2a
 Elastic Properties of U oxides, calculated using various functionals as indicated.

Property	UO ₂	UO ₂	UO ₂	UO ₂	UO ₂	
(in GPa)	Calculated	Calculated	Experiment	Calculated	Calculated CASTEP	
Indicated by	CASTEP	CASTEP	[20]	CASTEP	(LDA +U)	
# quantity:	[5]	[10]		(LDA +U)	U = 3.5 eV	
unit less	(GGA/PBE)	(LDA)		U = 2 eV	Stress fit	Energy fit
B	170.1	229.1	208.9	214.2	212.5	216.4
G	70.3 (G _v)	104.9		86.64	83.3	92.7
G/B [#]	0.41	0.46		0.40	0.39	0.43
	(G _v /B _v)					

Y ($Y_{[100]}$)	185.4 (Y_v)	273.0 (342.9)		228.9 (316.5)	221.3 (299.7)	179.6
c_{11}	318.2	411.9 (± 1.7)	389.3	353.9 (± 0.6)	370.5 (± 21.7)	393.5
c_{12}	96.0	137.7 (± 0.4)	118.7	91.2 (± 1.5)	133.6 (± 10.4)	127.8
c_{44}	43.1	87.6 (± 1.2)	59.7	65.1 (± 1.6)	65.5 (± 10.4)	65.9
$n^\#$		0.25		0.20	0.27	

The intrinsic brittleness, calculated according to Cottrell’s prescription (G/B) [24] does not show much variation with the changes in composition by substituting U by Th or Pu.

The good agreement between the calculated and experimental elastic moduli [22, 23] of ThO₂ was obtained (see Table 2b).

Table 2b
 Elastic Properties of U-Th-Pu oxides, calculated using LDA.

Property (in GPa) Indicated by # quantity: unit less	PuU ₃ O ₈ Calculated CASTEP (LDA)	ThO ₂ Calculated CASTEP (LDA)	ThO ₂ Experiment (fully dense)
B	224.7	213.4	193 [22]
G	102.1	102.2	100.1, 100.8 [23] 97.2 [22]
G/B [#]	0.45	0.48	
Y ($Y_{[100]}$)	265.9 (339.5)	264.4 (321.5)	262.1, 260.6 [23] 247.7 [22]
c_{11}	406.0 (± 1.1)	385.0 (± 1.2)	
c_{12}	134.1 (± 1.2)	127.6 (± 0.7)	
c_{44}	84.1 (± 1.7)	87.5 (± 0.3)	
$n^\#$	0.25	0.25	0.301 [23] 0.284 [22]

4. Thermal expansion

We examined the thermal expansion of thoria and urania for which experimental results are available. Preliminary first principles molecular dynamics simulations were performed using Andersen-Hoover barostat [25,26]. The calculations were performed for selected temperatures (starting at 300 K) and constant pressure [27] (1 atm). Running averages of the relative (versus the calculated room temperature value) change of the lattice constant of thoria, simulated by CASTEP (LDA) molecular dynamics as a function of temperature are shown in Fig. 6. The small unit cells shown in Fig. 1 were used, therefore large thermal fluctuations

were observed at higher temperatures. The calculated thermal expansion of thoria agrees with experimental data [28-31].

The relative thermal expansion of urania is calculated versus the lattice constant at room temperature obtained by the linear fit (shown by dotted line in Fig. 7) to CASTEP (LDA + U (3.5 eV)) results, because of larger scattering of the obtained values than for ThO₂.as. The simulated relative changes of the lattice constants of urania as a function of temperature are also in good agreement with the Fink values (shown by solid line) of thermal expansion of urania fuel [32]. Although more elaborated simulations for larger unit cells are needed to determine thermal expansion accurately, preliminary results shown in Fig.7 indicate that CASTEP (LDA + U (3.5 eV)) predicts slightly larger expansion of urania (indicated by triangles) than thoria (squares, LDA scheme). The results for thoria agree well with the recent measurements for slightly diluted thoria with urania (3.75%) [33]. The new experimental results [33] also indicate lower thermal expansion for thoria than urania [32].

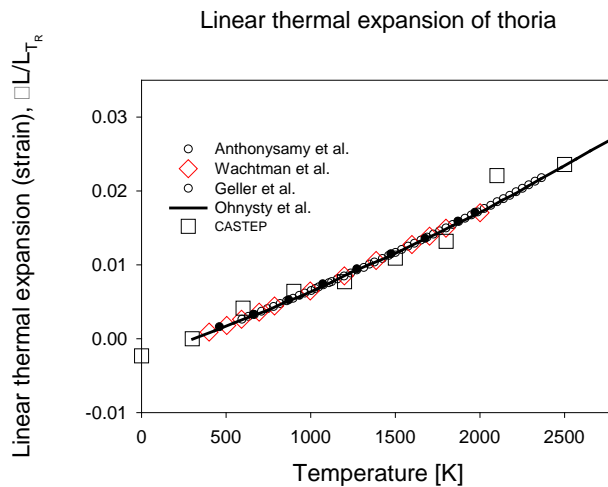


Figure 6 CASTEP (LDA) molecular dynamics simulation of relative linear thermal expansion of thoria (large squares) versus experimental data as indicated [28-31].

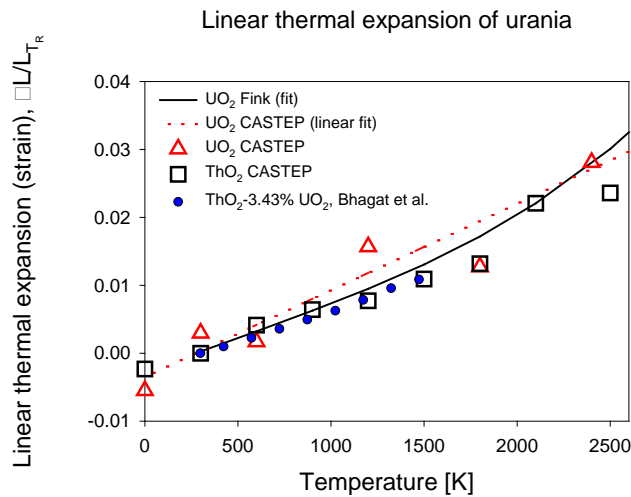


Figure 7 CASTEP molecular dynamics simulation of urania (triangles) and thoria (squares) versus experimental data as indicated [32,33]. The linear fit to the calculated by CASTEP (LDA + U (3.5 eV)) results for uranis is shown by dashed line.

5. Application

The presented, calculated values of elastic moduli were done at 0 K and therefore represent zero point maximum values since as described in [33] their values decrease with increasing temperature. We repeated the calculations [11, 12] of elastic moduli of U_3O_8 and urania expansion during oxidation using LDA + U (2eV). The stress strain gradients for the elastic moduli of U_3O_8 have been calculated using LDA+U geometries but with Hubbard term omitted. Using the Young Modulus calculated at 0 K (shown in Table 3 in the first column) and calculated relative volume expansion: 0.36, one can estimate the pressure on the sheath in which the immersed fuel oxidised to U_3O_8 . The pressure is independent on the size of container, but it varies with shape, as shown in Table 3. More details about these calculations can be found in [11, 12].

Table 3 - Calculated stress in the fuel sheath for urania oxidised to U_3O_8 .

Young Modulus [GPa]	Stress [GPa]		
	Sphere or equiaxial cylinder Strain: 0.10793	Long cylinder Strain: 0.16619	Plane Strain: 0.36
187.5 (random texture)	20.24	31.16	67.50
177.0 (x, y)	19.10	29.42	63.72
552.5 (z)	59.63	91.82	198.90

6. Conclusion

The CASTEP *first-principles* quantum mechanical program, employing density functional theory, is used to calculate elastic, magnetic and structural properties of U-Th-Pu oxides.

Detailed *first-principles* calculations enhance understanding of the properties of these oxides and allow predicting structure and properties in agreement with available experiments. Such calculations can be used to predict the properties of novel complex fuels and can become an important tool for modeling the properties of recycled fuels.

- **Acknowledgement**

The access to high performance supercomputers at CLUMEQ, Mammoth and Westgrid is acknowledged. This work was done partially in collaboration with A. Goldberg from Accelrys, Inc.. The helpful comments by V. Milman are also greatly appreciated.

7. References

- [1] P.G. Boczar, P.S.W. Chan, G.R. Dyck, R.J. Ellis, R.T. Jones, J.D. Sullivan, P. Taylor, “Thorium Fuel-Cycle Studies for CANDU Reactors”, IAEA-TECDO,1319 (1998) 25.
- [2] P.G. Boczar, J.T. Rogers and D.H. Lister, “Considerations in Recycling Used Natural Uranium Fuel from CANDU Reactors in Canada”, Proc. 31st Ann. Conf. of the Canadian Nuclear Society, Montreal, Canada, 24 - 27 May 2010, T1.
- [3] J.D. Sullivan and D.S. Cox, “AECL Progress in Developing the DUPIC Fuel Fabrication Process”, Proc. 4th Int. Conf. on CANDU fuel, Pembroke, Ontario, Canada, 1-4 October 1995, Vol. 2 4A-49-58.
- [4] M.D. Segall, P.L.D. Lindan, M.J. Probert, C.J. Pickard, P.J. Hasnip, S.J. Clark and J.D. Payne, “First-Principles Simulation: Ideas, Illustrations and the CASTEP Code”, J. Phys. Cond. Matt. 14 (2002) 2717-43.
- [5] C.J. Pickard, B. Winkler, R.K. Chen, M.C. Payne, M.H. Lee, J.S. Lin, J.A. White, V. Milman and D. Vanderbilt, “First-Principles Simulation: Ideas, Illustrations and the CASTEP Code”, Phys. Rev. Lett. 85 (2000) 5122-5.
- [6] B. Szpunar, J.A. Szpunar, “The Crystal Structure of pure and doped Urania”, Proc. CNS 6th Int. Conf. on Simulation Methods in Nuclear Engineering, Montreal, 13-15 October 2004, 3C.
- [7] J.P. Perdew, Y. Wang, “Accurate and simple analytic representation of the electron-gas correlation energy”, Phys. Rev. B45 (1992) 13244-49.
- [8] J.P. Perdew, K. Burke, M. Ernzerhof, “Generalized Gradient Approximation Made Simple”, Phys. Rev. Lett. 77 (1996) 3865-8.
- [9] M. Cococcioni, S. de Gironcoli, “Linear response approach to the calculation of the effective interaction parameters in the LDA+U method”, Phys. Rev. B71 (2005) 035105-16.
- [10] X. Zhao and D. Vanderbilt, “Phonons and lattice dielectric properties of zirconia”, Phys. Rev. B65 (2002) 075105-1-10.

- [11] B. Szpunar. and J.A. Szpunar, D. Oh., “Structural and Mechanical Properties of Urania Oxidized to U_3O_8 ”, Proc., 11th Int. Conf. on CANDU Fuel, Niagara Falls, Canada, 17-20 October 2010, T2.
- [12] B. Szpunar, J.A. Szpunar, “Theoretical Investigation of Structural and Mechanical Properties of Uranium Oxides”, Proc. 3rd Int. Conf. on Uranium, Uranium 2010, (ed. by E.K. Lam, J.W. Rowson, E. Özberk), Saskatoon, Canada, August 2010, Vol. II, 177.
- [13] B. Szpunar and J.A Szpunar, “The Crystal structure and Elastic Properties of Pure and Dy Doped Urania.”, Proc. The 30th Annual Conference of the Canadian Nuclear Society, Calgary, Canada, 31st May – 3rd June 2009, T3.
- [14] D.M. Ceperley, B.J. Alder, “Ground State of the Electron Gas by a Stochastic Method”, Phys. Rev. Lett. 45 (1980) 566-9.
- [15] R.W.G . Wyckoff, Crystal Structures, 2nd Ed., John Wiley & Sons, Inc., New York, 1963 vol. 2, pp. 467.
- [16] A.A. Sviridova and N.V. Suikovskaya, "Transparent limits of interference films of hafnium and thorium oxides in the ultraviolet region of the spectrum," Opt. Spectrosk. 22, (1967) 509-512 (orig. in Russ: 22 (1965) 940).
- [17] Y. Baer and J. Schoenes, “Electronic structure and Coulomb correlation energy in UO_2 single crystal”, Solid State Commun. 33 (1980) 885-8.
- [18] A. Reuss, “Electronic structure and Coulomb correlation energy in UO_2 single crystal “, Z. Angew. Math. Mech. 9 (1929) 49-58.
- [19] W. Voigt Lehrbuch der Krystallphysik, Ed. by B.G. Teubner, Leipzig, 1928, pp. 962.
- [20] I.J. Fritz, “Elastic properties of UO_2 at high pressure“, J., Appl. Phys. 47 (1976) 4353-7.
- [21] B. Szpunar, “Investigation of urania within LDA+U method” J. Phys. Chem. Solids 73 (2012) 1003-9.
- [22] K.K. Phani, D. Sanyal, “Elastic properties of porous polycrystalline thoria—A relook”, J. Eur. Ceram. Soc. 29 (2009) 385-90.
- [23] K.K. Phani, “Elastic-constant-porosity relations for polycrystalline thoria”, J. Matt. Sc. Lett. 5 (1986), 747-50.
- [24] Electron Theory in Alloy Design, Ed. by D.G. Pettifor and A.H. Cottrell, Maney Materials Science, London, 1992 (see p. 284).
- [25] H. C. Andersen, "Molecular dynamics simulations at constant pressure and/or temperature", J. Chem. Phys., 72 (1980) 2384- 2393.
- [26] Hoover, W. "Canonical dynamics: Equilibrium phase-space distributions", Phys. Rev. A, 31 (1985) 1695-1697.
- [27] S. Nosé, "Constant temperature molecular dynamics methods", Prog. Theor. Phys., Suppl., 103 (1991) 1-46.

- [28] S Anthonysamy, G Panneerselvam, S Bera, S.V. Narasimhan, P.R. Vasudeva-Rao, “Studies on thermal expansion and XPS of urania-thoria solid solutions”, J. Nucl. Mat. 281 (2000)15-21.
- [29] J.B. Wachtman Jr, T.G. Scuderi, G.W. Cleek “Linear thermal expansion of aluminum oxide and thorium oxide from 100 to 1100 K”, J. Am. Ceram. Soc. 45 (1962) 319-320.
- [30] R.F. Geller and P.J. Yavorsky, “Effects of Some Oxide Additions on Thermal-Length Changes of Zirconia”, J. Res. Natl. Bur. Std., 35 [1] 87-110 (1945); RP 1662; Ceram. Abstr., 24 [10] 191 (1945) (Reproduced from Ref. [30]).
- [31] B. Ohnysty and F.K. Rose, “Thermal Expansion Measurements on Thoria and Hafnia to 4500°F”, J. Am. Ceram. Soc. 47 (1964) 398-400.
- [32] S.G. Popov, J.J. Carbajo, V.K. Ivanov, G.L. Yoder, “Thermophysical Properties of MOX and UO₂ Fuels Including Effects of Irradiation”, ORNL/TM-2000/351, pp. 48.
- [33] R.K. Bhagat, K. Krishnan, T.R.G. Kutty, Arun Kumar, H.S. Kamath, S. Banerjee, “Thermal expansion of simulated thoria–urania fuel by high temperature XRD”, J. Nucl. Mat., 422 (2012) 152-157.
- [34] H. Ledbetter, “Sound velocities, elastic constants: Temperature dependence”, Materials Science and Engineering A 442 (2006) 31-34.